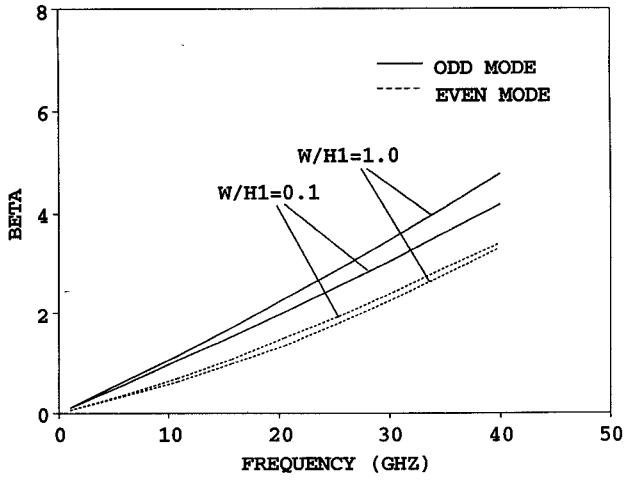

Fig. 8. Propagation constant versus frequency of lines on lithium niobate with $b = 4.318$ mm, $h_1 = 0.254$ mm, $h_2 = 5.08$ mm, $\epsilon_{xx} = 43.0$, $\epsilon_{yy} = \epsilon_{zz} = 28.0$, and $\mu_{xx} = \mu_{yy} = \mu_{zz} = 1.0$.

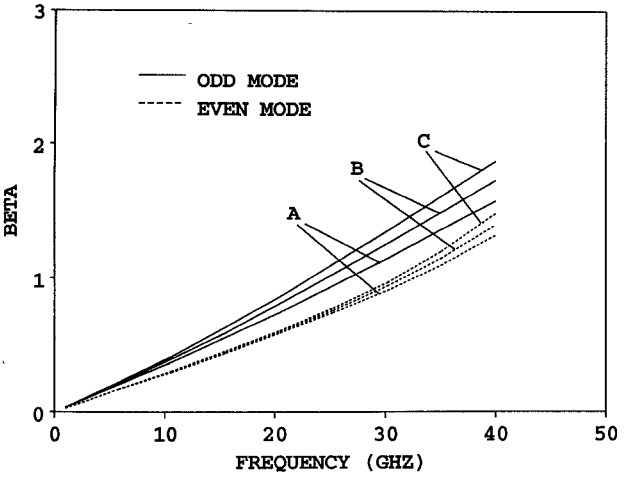

Fig. 9. Propagation constant versus frequency of lines on substrate characterized by $\epsilon_{xx} = 2.0$, $\epsilon_{yy} = 2.35$, and $\epsilon_{zz} = 3.50$ with $b = 4.318$ mm, $h_1 = 0.50$ mm, $h_2 = 4.834$ mm, and $w = 0.5$ mm. A: $\mu_{xx} = 2.75$, $\mu_{yy} = 2.25$, $\mu_{zz} = 5.00$. B: $\mu_{xx} = 3.25$, $\mu_{yy} = 2.75$, $\mu_{zz} = 5.50$. C: $\mu_{xx} = 3.75$, $\mu_{yy} = 3.25$, $\mu_{zz} = 6.00$.

10.0 GHz. The results of this study indicate that anisotropy, whether electric or magnetic, is important and cannot be neglected, especially at higher frequencies.

IV. Conclusion

A rigorous analysis through an application of the spectral-domain technique for a broadside coupled microstrip line on anisotropic substrates has been presented. The new expressions for the Green's functions for both the even and odd modes are derived via the transformed fourth-order differential equations. The numerical solution is obtained by using the Galerkin method in the Fourier domain. Numerical data for the effective dielectric constant computed by this method agree well with those previously published for the special case of isotropic substrate. Effects of anisotropy on shielded lines along the E-plane direction of the waveguide printed on different uniaxial and biaxial substrates are studied with respect to different strip widths. It is observed that generally, for all treated cases, the odd-mode effective dielectric constant is much more sensitive to changes in the strip width than that for the even mode, especially when higher values are selected for the elements of the $[\epsilon]$ tensor. Finally, dispersion curves for both magnetically and dielectrically anisotropic substrates are also generated to illustrate their effects on the propagation constant of the broadside coupled line.

References

[1] J. L. Allen and M. F. Estes, "Broadside coupled strips in a layered dielectric medium," *IEEE Trans. Microwave Theory Tech.*, vol. MTT-20, pp. 662–669, Oct. 1972.

[2] J. Bornemann, "Anwendung der methode der orthogonalreihenentwicklung auf quasiplanaare structuren mit homogenem und inhomogenem dielecktrikum," Ph.D. thesis, Univ. of Bremen, West Germany, 1984.

[3] H. Mizuno, C. J. Verver, R. J. Douville, and M. G. Stubbs, "Propagation in broadside coupled suspended-substrate stripline in E-plane," *IEEE Trans. Microwave Theory Tech.*, vol. MTT-33, pp. 946–951, Oct. 1985.

[4] N. G. Alexopoulos, "Integrated Circuit structures on anisotropic substrates," *IEEE Trans. Microwave Theory Tech.*, vol. MTT-33, pp. 847–881, Oct. 1985.

[5] A. G. D'Assunçao, A. J. Giarola, and D. A. Rogers, "Characteristics of broadside coupled microstrip lines with iso/anisotropic substrates," *Electron. Lett.*, vol. 17, no. 7, pp. 264–265, Apr. 1981.

[6] S. K. Koul and B. Bhat, "Transverse transmission line method for the analysis of broadside coupled microstrip lines with anisotropic substrates," *Arch. Elek. Übertragung.*, vol. 37, pp. 59–64, Jan./Feb. 1983.

[7] T. Q. Ho and B. Beker, "Spectral-domain analysis of shielded microstrip lines on biaxially anisotropic substrates," pp. 1017–1021, this issue.

[8] L. P. Schmidt and T. Itoh, "Spectral domain analysis of dominant and higher order modes in finline," *IEEE Trans. Microwave Theory Tech.*, vol. MTT-28, pp. 981–985, Sept. 1980.

[9] T. Itoh and R. Mittra, "Spectral domain approach for calculating the dispersion characteristics of microstrip lines," *IEEE Trans. Microwave Theory Tech.*, vol. MTT-21, pp. 496–499, July 1973.

[10] T. Itoh, "Analysis of microstrip resonators," *IEEE Trans. Microwave Theory Tech.*, vol. MTT-22, pp. 946–952, Nov. 1974.

[11] Y. C. Shih and T. Itoh, "Analysis of transmission lines on semiconductor substrate," Univ. of Texas Microwave Laboratory Rep. No. 84-2, Mar. 1984.

Picosecond Pulse Propagation in Coplanar Waveguide Forward Directional Couplers

P. Singkornrat and J. A. Buck

Abstract—**The spectral-domain method is used to calculate the frequency-dependent even- and odd-mode effective dielectric constants of symmetric coplanar waveguide forward directional couplers. Comparisons are made with symmetric microstrip forward couplers on the same substrate that have the same line spacing and access port characteristic impedance. Results indicate that certain coplanar designs will have lower loss and greater bandwidth than the microstrip devices. Picosecond pulse propagation in both structures is studied using the calculated dispersion data.**

Manuscript received May 3, 1990; revised January 22, 1991. This work was supported by IBM Boca Raton through the IBM Resident Study Program.

The authors are with the School of Electrical Engineering, Georgia Institute of Technology, Atlanta, GA 30332.

IEEE Log Number 9144280.

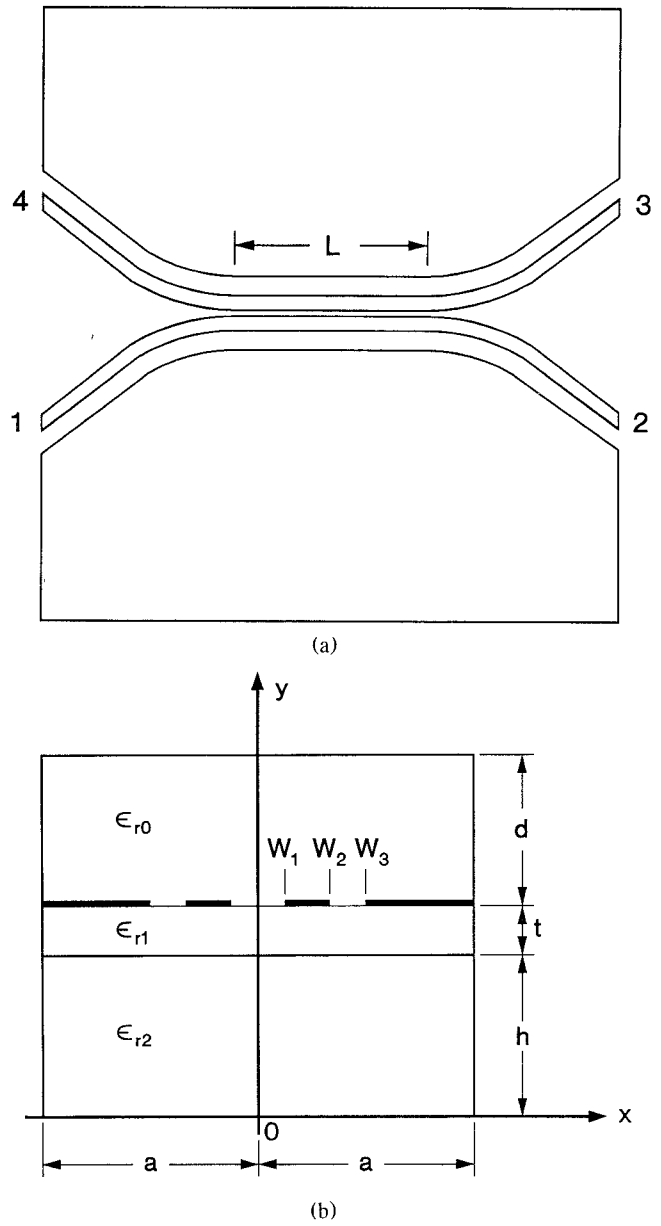

Fig. 1. Coplanar waveguide forward directional coupler: (a) top view; (b) cross section.

I. Introduction

Forward-coupling microstrip hybrids have recently been shown to be attractive for broad-band coupling applications; bandwidths of up to 57% have been achieved using asymmetric designs [1]. Another recent experiment demonstrated a sequential waveform generation scheme using a forward microstrip coupler that was optoelectronically triggered by picosecond light pulses [2]. All such devices consist of two closely spaced lines, the ends of which are impedance-matched to the output ports through curved line sections that provide tapered spacing (Fig. 1). Coupling between the lines can be understood by considering the electric field distribution as two quasi-TEM modes having even and odd symmetries (see [3] for electric field configurations). An input voltage wave at port 1 will cross over to port 3 by means of a phase shift that accumulates between the even and odd modes as they propagate at different velocities down the length of the coupling region. Complete power crossover can occur during a single transit.

The present study concerns the use of coplanar waveguide geometry in the construction of forward couplers and the propagation of short pulses in these structures. It is shown that advantages over microstrip include greater bandwidth and lower conductor loss in some designs. The effective even- and odd-mode dielectric constants are calculated using the spectral-domain method in a manner similar to that of Davies *et al.* [4]. Propagation and dispersion of picosecond pulses are studied by a fast Fourier transform calculation that obtains the outputs at the direct and crossover ports.

II. Dispersion and Coupling

The coupler geometry is shown in Fig. 1. To reduce computation time, a rectangular metallic shield is assumed to surround the coupler. This allows the use of discrete summations, as opposed to the required integrations that would appear without the shield. The open structure can be closely approximated if the dimensions of the shield are large compared with the widths of the lines and gaps [5], [6]. Coupling between the curved sections is assumed negligible; only the straight coupling section of length L is considered.

In the spectral-domain method, the boundary conditions at $y = h$ and $y = h + t$ and the requirement of zero electric field at the top and bottom shields are used to obtain the spectral domain equation.

$$\begin{bmatrix} G_{11} & G_{12} \\ G_{21} & G_{22} \end{bmatrix} \begin{bmatrix} \tilde{J}_x \\ \tilde{J}_z \end{bmatrix} = \begin{bmatrix} \tilde{E}_z \\ \tilde{E}_x \end{bmatrix} \tag{1}$$

where G_{ij} are the elements of the dyadic Green's function in the spectral domain [4], [7]. $\tilde{J}_x$ and $\tilde{J}_z$ are the transforms of the transverse and longitudinal currents, respectively. In many studies the procedure at this stage is to assume a current distribution and to solve for the propagation constants using (1). In the present device it is more accurate to approximate the electric fields in the regions between conductors and use the inverse of (1). The electric fields must be chosen such that they are zero on the strips and nonzero in the gaps. Longitudinal fields (E_z) are assumed zero since their contributions to the effective dielectric constants are not significant over the frequency range to be considered [6]. The following closed-form expressions for the electric field distributions are used:

$$E_{x1} = \frac{-1}{2W_1}\left[3\left(\frac{x}{W_1}\right)^2 + 1\right], \qquad 0 < |x| < W_1 \tag{2}$$

$$E_{x1} = \frac{1}{2S}\left[3\left(\frac{|x| - W_2 - S}{S}\right)^2 + 1\right], \qquad W_2 < |x| < W_3 \tag{3}$$

for the odd mode and

$$E_{x1} = \frac{-x}{2W_1^2}\left[3\left(\frac{x}{W_1}\right)^2 + 1\right], \qquad 0 < |x| < W_1 \tag{4}$$

$$E_{x1} = \frac{x}{2S|x|}\left[3\left(\frac{|x| - W_2 - S}{S}\right)^2 + 1\right], \qquad W_2 < |x| < W_3 \tag{5}$$

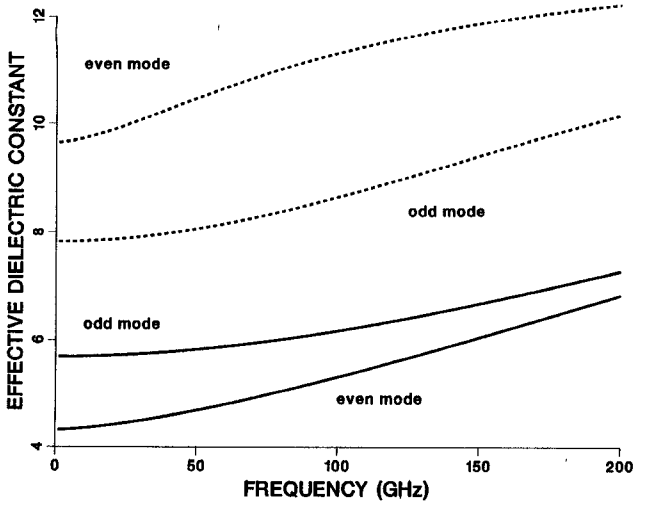

Fig. 2. Effective odd- and even-mode dielectric constants of a coplanar waveguide coupler (solid lines) and a microstrip coupler (dashed lines). Both devices have access ports with 50 Ω characteristic impedance.

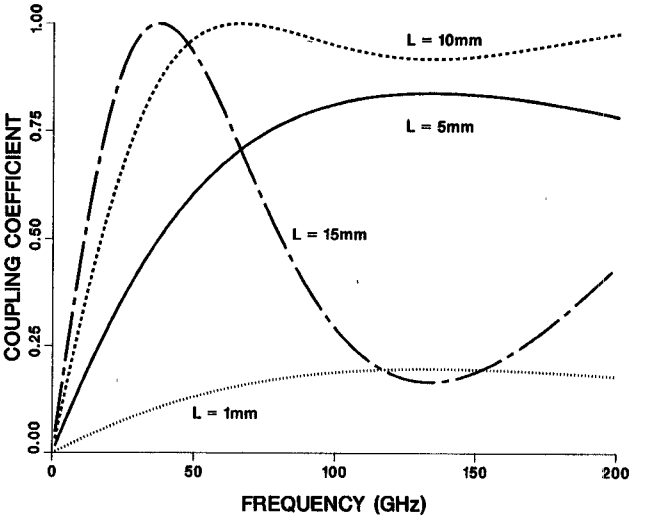

Fig. 3. Coupling coefficients ($|S_{31}|$) for the coplanar waveguide coupler having effective dielectric constants as shown in Fig. 2.

for the even mode, where $2S = W_3 - W_2$. These expressions are similar to those used in [5] except that allowance is made in this work for different values of W_1/S.

The effective dielectric constants of a coplanar forward coupler with 50Ω access ports on a 100-μm-thick GaAs ($\epsilon_r = 13.2$) substrate were calculated and are plotted in Fig. 2. This substrate thickness was selected to minimize radiation and higher order mode losses at higher frequencies. According to [8], a conservative guideline to avoid all potential problems is to operate below the cutoff frequency of the TE_0 mode; i.e., the substrate thickness should be less than $0.12\lambda_d$, where λ_d is the dielectric wavelength. Since the GaAs substrate is 100 μm thick, frequencies should be equal to or less than 100 GHz. Specifications of the coupler are $\epsilon_{r0} = \epsilon_{r2} = 1$, $\epsilon_{r1} = 13.2$, $a = 10$ mm, $d = 10$ mm, $t = 100$ μm, $h + t = 10$ mm, $W_1 = 15$ μm, $W_2 = 225$ μm, and $W_3 = 325$ μm. For comparison, the dielectric constants of a microstrip coupler with 50 Ω access ports on a GaAs substrate of the same thickness were also calculated using the spectral-domain method. These results are shown in the same figure. Both couplers have the same line impedance and 30 μm gap separating the two lines so that coupling and pulse propagation characteristics can be compared. Conductor losses for both structures were calculated using [3, eqs. (2.133) and (7.32)]. For 1-μm-thick gold lines, the coplanar coupler has a conductor loss of 0.6 dB/cm at 100 GHz while the microstrip coupler has a conductor loss of 1.4 dB/cm at that frequency.

It is seen in Fig. 2 that over the frequency range considered, the difference between odd- and even-mode dielectric constants in the coplanar coupler is lower than in the microstrip coupler. This arises from the greater similarity in the odd- and even-mode electric field configurations in the coplanar device. Furthermore, the difference between the dielectric constants in the microstrip coupler increases with frequency over the lower half of the frequency range, whereas the corresponding difference in the coplanar coupler decreases with frequency over the entire range. The significance of this is seen when considering the crossover efficiency between ports 1 and 3, given by the coupling coefficient [1],

$$S_{31} = -i \sin\left(\frac{\pi \Delta n_{\text{eff}} L}{c} f\right) \tag{6}$$

where f is the frequency, c is the speed of light in vacuum, and Δn_{eff} is the difference between the square roots of the odd- and even-mode dielectric constants. The smooth decrease in Δn_{eff} with frequency for the coplanar waveguide structure provides a qualitative indication that S_{31} can experience little change over a broad frequency range. This is evident in Fig. 3, where the coupling coefficients of the coplanar device for various lengths are plotted. At 10 mm the coupling coefficient is almost unity for a wide range of frequencies. This arises from the decreasing difference between odd- and even-mode dielectric constants as frequency is increased, thus slowing the variation of S_{31}, as can be seen by inspection of (6). For the microstrip device, complete crossover at a given frequency is achieved over a shorter length than in the coplanar device because of a larger difference between the dielectric constants. However, the microstrip coupler bandwidth is narrower than that of the coplanar coupler, since the microstrip Δn_{eff} either increases or remains relatively constant as the frequency is raised.

In the coplanar coupler, Δn_{eff} was found to decrease with increasing frequency if $t/(W_2 - W_1)$ is less that 2, $W_1/(W_3 - W_2)$ is less than 0.5, and the upper frequency limit is below twice the TE_0 mode cutoff frequency. This is in agreement with the data reported in [5]. In the microstrip coupler, Δn_{eff} always increases with increasing frequency in the lower frequency range.

III. Propagation of Picosecond Pulses

To study the behavior of both the coplanar waveguide and microstrip couplers under pulsed operation, a computational routine was performed in which a Gaussian input pulse at port 1 was propagated to the outputs at ports 2 and 3 according to the dispersion models formulated in Section II. The input pulse assumes the form $V(0,t) = V_{0\exp}[-(4\ln 2)t^2/\tau^2]$, where τ is the full width at half maximum of the pulse. The pulse is Fourier transformed and split into even and odd modes as in [9] so that, at the input, $V(0,\omega) = V_e(0,\omega) + V_o(0,\omega)$. After propagating through a length, L, the Fourier transform of the pulse becomes

$$V(L,\omega) = V_e(0,\omega)e^{-i\beta_e(\omega)L} + V_o(0,\omega)e^{-i\beta_o(\omega)L} \tag{7}$$

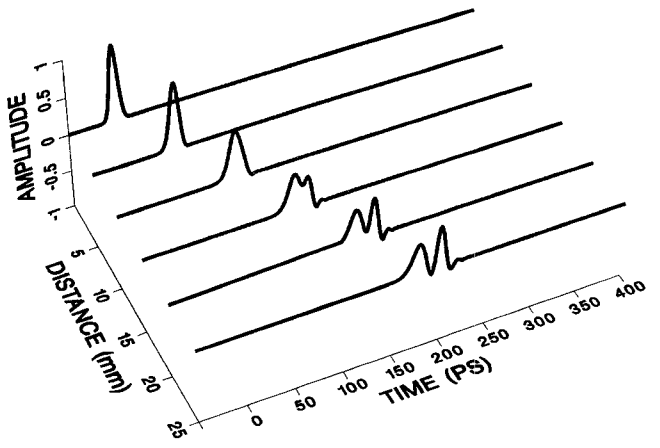

(a)

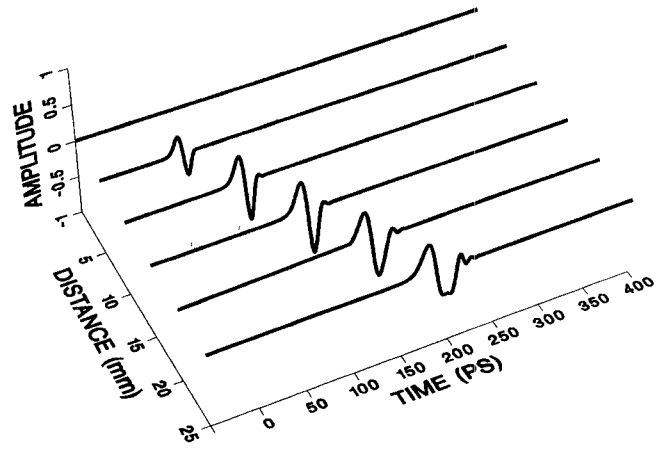

(b)

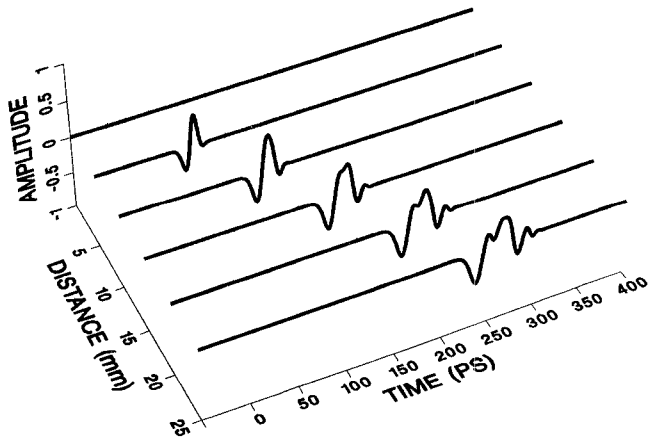

(c)

Fig. 4. Responses of the coplanar waveguide and microstrip couplers to a 10 ps input pulse: (a) coplanar waveguide direct port; (b) coplanar waveguide crossover port; (c) microstrip crossover port.

where $\beta_e(\omega) = \omega / c\sqrt{\epsilon^e_{\text{reff}}(\omega)}$ and $\beta_o(\omega) = \omega / c\sqrt{\epsilon^o_{\text{reff}}(\omega)}$. The outputs at port 2 (direct port) and port 3 (crossover port) are given by

$$V_2(\omega) = \frac{1}{2} V(0,\omega)\{e^{-\iota\beta_e(\omega)L} + e^{-\iota\beta_o(\omega)L}\} \tag{8}$$

$$V_3(\omega) = \frac{1}{2} V(0,\omega)\{e^{-\iota\beta_e(\omega)L} - e^{-\iota\beta_o(\omega)L}\}. \tag{9}$$

The inverse transforms of $V_2(\omega)$ and $V_3(\omega)$ give the time-dependent output pulses at the direct and crossover ports, respectively.

A 10 ps FWHM Gaussian pulse was input to port 1 of both couplers. Conductor losses were neglected because their influence on this pulse is small. The resulting waveforms at the direct and crossover ports for various coupler lengths were calculated and are shown in Fig. 4. At 5 mm, the crossover response of the microstrip coupler is larger than that of the coplanar coupler, as a result of a larger coupler coefficient. At 10 mm, the waveforms at port 3 for both couplers have almost the same amplitude and width. At 15 mm, the coplanar coupler output pulse exhibits a larger amplitude and is narrower.

IV. Conclusion

The spectral-domain method was used to calculate the effective odd- and even-mode dielectric constants of coplanar waveguide and microstrip forward-coupling structures. Coupling and dispersion of a 10 ps Gaussian pulse were computed in selected structures. It was shown that when compared with a microstrip coupler on an identical substrate a coplanar waveguide coupler can be designed to have less conductor loss and greater bandwidth and can produce less pulse distortion.

Acknowledgment

The authors acknowledge helpful discussions with G. S. Smith.

References

[1] P. Ikalainen and G. L. Matthaei, "Wide-band, forward-coupling microstrip hybrids with high directivity," *IEEE Trans. Microwave Theory Tech.*, vol. MTT-35, pp. 719–725, Aug. 1987.

[2] J. A. Buck, M. A. Neifeld, and M. W. Bowers, "Optoelectronic sequential waveform generation in a microstrip directional coupler," *J. Appl. Phys.*, vol. 63, pp. 2162–2164, Mar. 1988.

[3] K. C. Gupta, R. Garg, and I. J. Bahl, *Microstrip Lines and Slotlines*. Norwood, MA: Artech House, 1979.

[4] J. B. Davies and D. Mirshekar-Syahkal, "Spectral domain solution of arbitrary coplanar transmission line with multilayer substrate," *IEEE Trans. Microwave Theory Tech.*, vol. MTT-25, pp. 143–146, Feb. 1977.

[5] D. Mirshekar-Syahkal, "Dispersion in shielded coupled coplanar waveguides," *Electron. Lett.*, vol. 22, pp. 358–360, Mar. 1986.

[6] T. Leung and C. A. Balanis, "Pulse dispersion distortion in open and shielded microstrips using the spectral-domain method," *IEEE Trans. Microwave Theory Tech.*, vol. 36, pp. 1223–1226, July 1988.

[7] T. Itoh and R. Mittra, "A technique for computing dispersion characteristics of shielded microstrip lines," *IEEE Trans. Microwave Theory Tech.*, vol. MTT-22, pp. 896–898, Oct. 1974.

[8] M. Riaziat, R. Majidi-ahy, and I. Feng, "Propagation modes and dispersion characteristics of coplanar waveguides," *IEEE Trans. Microwave Theory Tech.*, vol. 38, pp. 245–251, Mar. 1990.

[9] J. P. Gilb and C. A. Balanis, "Pulse distortion on multilayer coupled microstrip lines," *IEEE Trans. Microwave Theory Tech.*, vol. 37, pp. 1620–1628, Oct. 1989.